Quantum Electronics **30** (8) 664 – 668 (2000)

LASERS

PACS numbers: 42.55.Px; 42.60.Jf
DOI: 10.1070/QE2000v030n08ABEH001787

Optical gain in InAs/InGaAs quantum-dot structures: Experiments and theoretical model

P G Eliseev, H Li, G T Liu, A Stintz, T C Newell, L E Lester, K J Malloy

Abstract. The dependence of the mode optical gain on current in InAs/InGaAs quantum-dot structures grown by the method of molecular-beam epitaxy is obtained from the experimental study of ultra-low-threshold laser diodes. The record lowest inversion threshold at room temperature was about 13 A cm^{-2}. A theoretical model is proposed that relates the optical gain to the ground-state transitions in quantum dots. The effective gain cross section is estimated to be $\sim 7 \times 10^{-15}$ cm^{-2}.

1. Introduction

Quantum-dimensional structures with a reduced dimensionality offer certain advantages in a number of applications [1, 2]. Quantum-dot (QD) laser diodes possess the lowest lasing threshold in the active region among all the room-temperature semiconductor lasers [3 – 6]. In DWELL (dot-in-a-well) structures with the InGaAs quantum well in the active region containing one layer of self-organised InAs dots, the threshold current density as high as 26 A cm^{-2} has been obtained [5].

Each QD represents an atom-like object with a discrete energy spectrum. The interband emission of a QD with the lowest energy, which is called the ground-state emission, corresponds to the transitions between the ground state of an electron in conduction-band well and the ground state of a hole in the valence-band well (Fig. 1). We will use this notation for a long-wavelength emission band of a QD, which provides the achievement of the lowest threshold.

If the current density is sufficiently high but lasing is absent (because of high optical losses in the diode cavity), emission and gain appear in the spectral bands of the so-called excited states located at higher energies. For example, DWELL lasers with uncoated faces [6] produce emission in the ground-state band at about 1 eV only in long (longer than 1.5 mm) cavities. The first excited band corresponds to the energy 1.07 eV.

The dependences of the emission intensity and optical gain on the current are important characteristics of QD lasers. In this paper, we present the results of our experimental studies and a model based on the rate equations, which describes the concentration of carriers in a QD and a surrounding quantum well. We found the relation between the carrier concentration in the ground state and the injection current density and also calculated the mode gain for a low pump level taking into account the effective gain cross section and the calculated optical limitation factor. The results of our simulation well agree with experimental dependences of the threshold gain on current, which were obtained for three different types of ultra-low-threshold QD lasers.

2. Samples and measurements

We studied ultra-low-threshold laser diodes with a broad (100 μm) cavity, which were made of three epitaxial InAs

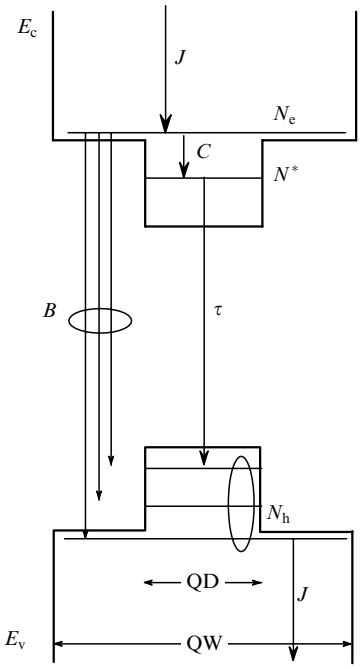

Figure 1. Energy transition diagram of a QD laser (the DWELL structure). The single upper and lower QD working levels are considered. The level notation: J are pump electronic transitions; C is a coefficient of the electron capture from a quantum well (QW) by a QD; τ are working transitions in the QD; B is a coefficient of parasitic recombination of electrons in the quantum well with holes in it and holes in the QD; and N^* is the concentration of the upper working state in the QD.

P G Eliseev P N Lebedev Physics Institute, Russian Academy of Sciences, Leninskii prosp. 53, 117924 Moscow, Russia
H Li, G T Liu, A Stintz, T C Newell, L E Lester, K J Malloy Center for High Technology Materials, University of New Mexico, 1313 Goddard, SE Albuquerque, NM 87106, USA

Received 23 March 2000
Kvantovaya Elektronika **30** (8) 664 – 668 (2000)
Translated by M N Sapozhnikov

Table 1. Parameters of the MBE structures studied.

Structure	M	d/nm	Two-dimensional QD density $/10^{10}$ cm^{-3}	Three-dimensional QD density $/10^{16}$ cm^{-3}	Fraction of In in a DWELL layer	λ/nm
SDWELL-577	1	10	2.5	2.5	0.15	1246
MDWELL-638	3	9.6	2.5	2.6	0.15	1250
SDWELL-432	1	10	7.5	7.5	0.20	1230

Note: M is the numer of DWELL layers in the structure; d is the thickness of a single DWELL layer; λ is the central wavelength of laser radiation.

QD structures overgrown in InGaAs quantum wells. Two of these structures contained single QD layers, while the third structure contained three active DWELL layer separated by GaAs layers 10 nm thick each. The corresponding data are presented in Table 1. The structures were grown by the molecular-beam epitaxy (MBE) method on GaAs substrates under conditions providing the self-organised growth of InAs QDs. Individual QDs had typical diameter of the base of about 15 nm and height of about 7 nm. The QD density was measured with an atomic-force microscope on parallel structures, which were not overgrown with materials of the quantum well and upper layers. The waveguide (GaAs) and active layers were undoped, while the $Al_{0.7}Ga_{0.3}As$ cover layer was doped with Be from the p side and with Si from the n side. The total waveguide thickness was 230 nm for all the structures.

Laser diodes with the cavity length between 285 and 7800 μm were manufactured from the processed structures by cleavage. The threshold current density and optical power of laser diodes with cavities of different length (with uncoated ends) were measured to obtain the coefficient of inner losses in each structure and the dependence of the mode gain on the current density. The lowest threshold density was 21 A cm^{-2} in a long diode made of structure 577 with cleaved faces and 16 A cm^{-2} in a diode with highly reflecting coatings on its ends. Other optical characteristics of laser diodes manufactured from these structures are presented in Refs [5, 6].

3. Experimental results

To obtain the dependence of the mode gain on the injection current density J, we measured the dependence of the threshold current on the cavity length L in laser diodes with a plane cavity. The external losses were calculated from a simple formula $(1/L)\ln(1/R)$, the Fresnel reflection coefficient R being taken for the semiconductor-air interface. The coefficient α_1 of inner optical losses was measured of the inverse external differential efficiency on L, which is close to a linear one in the region 4 mm $< L <$ 1 mm. The lowest value of α_1 equal to 1.3 cm^{-1} was obtained for lasers made of structure 432; for lasers made of structures 577 and 638, α_1 was 1.5 cm^{-1}.

Fig. 2 shows the dependences of the relative spectral density I of spontaneous emission and mode gain g_{mod} on the current density. The density of spontaneous emission saturates already above the current density equal to 30 A cm^{-2}. The mode gain is also substantially saturated. The solid curves describing these dependences were calculated using a theoretical model with fitting parameters that were the same for spontaneous emission and gain. The dependences of the mode gain on the current for diodes made of different epitaxial structures are shown in Fig. 3.

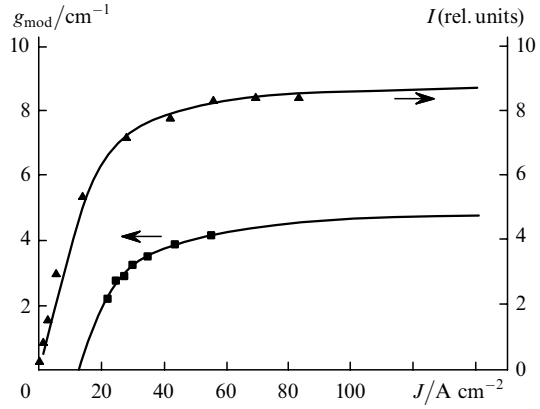

Figure 2. Dependences of the relative spectral density I of spontaneous emission and the mode gain g_{mod} on the current density for a DRWELL-577 sample. The curves are calculated dependences.

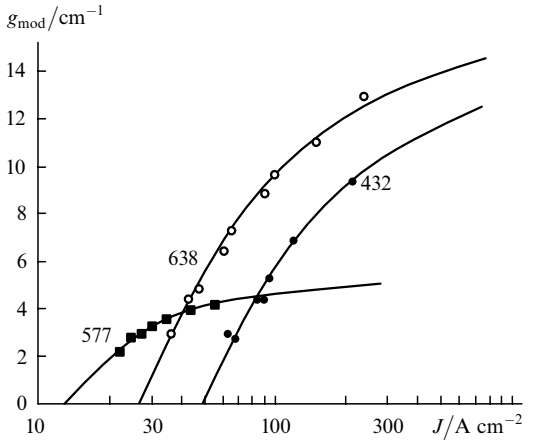

Figure 3. Dependences of the mode gain on the current density in QD lasers made of three epitaxial structures (the structure numbers are shown at the curves)

4. The gain model

4.1. Introductory comments

A detailed kinetic model involves many variables that represent concentrations of excess carriers in several states in QDs (including the ground and excited states, neutral and charged states), as well as in a quantum well and waveguide layers. Here, we are interested in the stationary populations of the electron (upper) and hole (lower) ground states, which contribute into lasing. We will restrict our model by a comparatively low pump level, which is sufficient for the complete inversion of the ground-state population. In this

case, the detailed distribution of excess carriers over higher energy states can be neglected.

We assume that these carriers reside in a bath (for certainty, in the electronic states in a quantum well) and can be accumulated there in a great amount. The electrons are captured from the bath to the upper QD state (a useful process) or recombine with any holes (a parasitic process). The stimulated emission in the ground-state band is caused only by the useful process. The effective capture coefficient C is introduced to describe the rate of the useful process (reverse emission of the electrons to the quantum well is also assumed but not calculated). All the recombination processes that do not contribute to the stimulated emission are described by the effective recombination coefficient B. These transitions are shown in Fig. 1.

The electrons captured by a QD populate the upper working state, which is characterised by a single lifetime τ. The concentration N^* of the upper working states is the most important quantity. We assume that holes easily populate the lower working state, so that the concentration of inverted QDs is N^*.

Thus, a positive gain is achieved when more than half the upper states available is populated by electrons. We do not consider the energy distribution over a broadened band of the ground states and the deviation of QDs from neutrality and also neglect the excess carriers in waveguide layers (assuming that the carriers flow directly to the quantum well). These simplifications seem to be justified for a low pump level but they should be reexamined in the case of an arbitrary pump level.

The gain of QD lasers has been also calculated by other methods [7–12]. Recently, the gain of a QD laser was calculated using the empirical approximation [12]

$$g(J) = g_0\left\{1 - \exp\left[-\frac{\gamma(J - J_0)}{J_0}\right]\right\}, \tag{1}$$

where g_0 is the maximum gain, γ and J_0 are fitting parameters (γ is a coefficient close to unity and J_0 is the inversion threshold). Our model based on the rate equations does not contradict to a more general random population (RP) model proposed in Ref. [10]. In our case, a bath containing carriers is located in the InGaAs quantum well, and only the ground-state population is calculated. The RP model was proposed for the description of the excited-state population, which is nonzero when the ground-state population is not saturated. In our model, a parasitic recombination channel includes recombination via the excited states, and a corresponding choice of the parameters results in the nonzero contribution of parasitic recombination.

4.2. Equations

We consider the rate equations for three variable concentrations: the QD concentration N^* in the upper working state, the electron concentration N_e in the quantum well, and the total hole concentration N_h in the active region. In addition, the following parameters were used: the QD concentration N^o in the lower working state; the total (three-dimensional) QD concentration N_{qd}; the lifetime τ of the upper state; the recombination coefficient B of electrons in the quantum well with all holes; the coefficient C of capture of electrons from the quantum well to the QD upper state; the quantum-well width d; and the injection current density J.

Our model assumes that N^* refer to active particles, and the decay of these particles corresponds to useful emission and gain. The parameters N_e and N_h describe carriers of both signs, which are not included into useful transitions, whose recombination corresponds to a parasitic channel of power losses. Here, we should note that this model allows us to interchange N_e and N_h. Therefore, we do not insist that it is the injected electrons that are shared between the working states (N^*) and the bath states (N_e). In principle, the injected holes can be shared in a similar way. The model also assumes that carriers of the same kind are shared between different states, which form competing decay channels.

The rate equations can be represented in the form

$$\begin{aligned}
\frac{dN^*}{dt} &= -\frac{N^*}{\tau} + CN_eN^o,\\
\frac{dN_e}{dt} &= \frac{J}{ed} - N_e(CN^o + BN_h),\\
\frac{dN_h}{dt} &= \frac{J}{ed} - BN_hN_e - \frac{N^*}{\tau}.
\end{aligned} \tag{2}$$

We consider stationary conditions ($d/dt = 0$) and assume that $N^* + N^o = N_{qd}$ (the only electronic state). To take into account the trend to the electric neutrality in the active region, we also assume that $N_e + N^* = N_h$. For convenience, we introduce normalised variables and parameters $z = N^*/N_{qd}$, $G = J\tau/(edN_{qd})$, $A = 1/(C\tau N_{qd})$, and $T = \tau BN_{qd}$. Note that z is a fraction of electrons in the upper state which can vary from zero (completely free states) to unity (completely occupied states). For τ fixed, a small value of T corresponds to a highly efficient laser. It is also preferable to have a small value of A, because in this case, the probability of particle capturing by QDs is great.

4.3. Solution

The stationary solution

$$G = z\left[1 + ATz(1 + A - z)/(1 - z)^2\right] \tag{3}$$

of the system of equations (2) has the following particular cases. For $G \ll 1$, the parameter $z \sim G$ (linear regime) and for $G \gg 1$, the parameter $z \sim 1$ (regime corresponding to the gain saturation when the gain asymptotically approaches its maximum value). The latter regime corresponds to a total inversion of the ground-state levels, so that all the QDs are in the upper state. The model takes into account that as the current further increases, the power is spent via other recombination mechanisms because the recombination via the ground state is saturated.

The calculated dependences of z on the relative pump rate are shown in Fig. 4. The value of z increases with G at small A and T up to $z \approx 1$ and then remains almost constant for $G > 1$. For large T, the curves are smoothed and z approaches unity at substantially larger values of G. Note that such behaviour is an intrinsic property of the QD population (beyond the stimulated emission regime) and is not related to the dynamic saturation during lasing. The equilibrium absorption in the ground-state band is σN_{qd}, where σ is the effective gain/absorption cross section of an individual QD. Therefore, the optical gain changes from $-\sigma N_{qd}$ for $z \approx 0$ to $\sim \sigma N_{qd}$ for $z \to 1$. The dependence of the gain on z can be written in the form

$$g(z) = 2\sigma N_{qd}(z - 0.5), \tag{4}$$

and inversion takes place for $z \geqslant 0.5$.

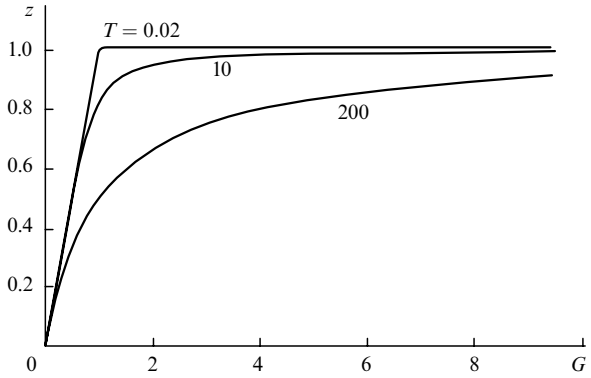

Figure 4. Calculated dependences of the relative concentration z of inverted QDs on the relative pump rate for $A = 0.005$ and $\tau = 1$ ns.

We will calculate the mode gain using the waveguide model and find the factor of optical limitation Γ for the quantum well by assuming that the material gain $g(z)$ produced by a QD is related to the entire quantum-well layer. In this case, the mode gain is

$$g_{\mathrm{mod}}(z) = \Gamma g(z). \tag{5}$$

For a single DWELL structure, the calculated value of $\Gamma = 0.0302$, and for the three-layer MDWELL structure, $\Gamma = 0.0906$. The dependence of the mode gain on the pump current was then calculated from Eqns (4) and (5) by substituting z from the numerical solution of Eqn (3). The calculations were fitted to the experimental results by using fitting parameters σ, A, and T.

Fig. 5 shows the calculated dependences of the normalised mode gain $\Gamma g(z)/(\sigma N_{\mathrm{qd}})$ on the relative pump rate. The curve shape and the inversion threshold depend on parameters A and T. The gain abruptly saturates at small values of A and T and slowly saturates at large values of A and T. The increase in these parameters corresponds to the increase of contribution from the parasitic recombination. Also, the dependence $1 - \exp[-(G-1)]$ is shown, which was earlier used for empirical fitting experimental data [12]. This curve describes the gain restriction with a rapid saturation, but it noticeably overestimates absorption for $G < 1$.

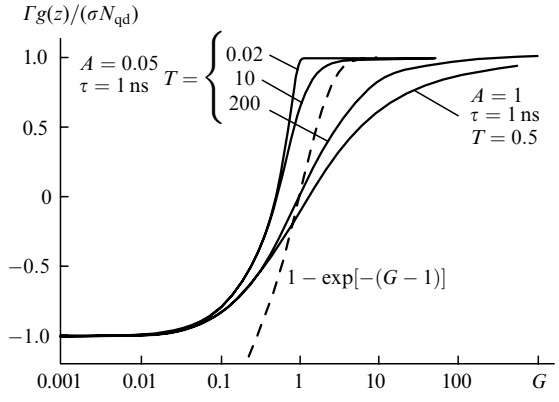

Figure 5. Calculated dependences of the relative gain $\Gamma g(z)/(\sigma N_{\mathrm{qd}})$ normalised to its maximum value on the relative pump rate G. $1-\exp[-(G-1)]$ is an empirical curve.

5. Discussion

By fitting the experimental data by calculated curves (Figs 2 and 3), we estimated the inversion threshold and the maximum gain produced by the QD ground states (Table 2). One can see that the minimum inversion threshold $J_0 = 13$ A cm^{-2} is achieved in laser diodes made of structure 577. As far as we know, this is the lowest threshold ever obtained for room-temperature semiconductor lasers. This structure provides a quite low mode gain (no more than 5.4 cm^{-1}), so that lasing in the ground-state band is achieved only in high-Q lasers with a long cavity or highly reflecting coatings.

Table 2. Parameters obtained from analysis of experimental data.

Structure	J_0/A/cm^{-2}	$g_{\max}$/cm^{-1}	$\sigma/10^{-15}$ cm^2	A	T
SDWELL-577	13	5.43	7.17	0.2	0.4
MDWELL-638	25.7	17	7.21	0.5	0.4
SDWELL-432	50	15.6	6.89	0.5	0.4

Note: $g_{\max}$ is the maximum mode gain.

A minimum inversion threshold obtained for this series of laser diodes by optimising mirrors was 16 A cm^{-2}. A higher gain was achieved in MDWELL-638 and SDWELL-432 structures with a high QD concentration. As the number of QDs in the active medium increases, the inversion and lasing thresholds increase. By using the calculated optical limitation factor, we determined the material gain in the quantum well produced by ground-state transitions. This gives an estimate of the effective gain cross section σ in a QD as $6.9 \times 10^{-15} - 7.2 \times 10^{-15}$ cm^2.

The parameters A and T of the kinetic model are also presented in Table 2. The coefficient C was estimated from A to be $(2 \pm 0.6) \times 10^{-7}$ cm^3 c^{-1}. This corresponds to the electron capture time of about 200 ps upon weak pumping and for $N_{\mathrm{gd}} = 2.5 \times 10^{16}$ cm^{-3}. The coefficient of parasitic recombination was estimated as $B = (2.6 \pm 0.6) \times 10^{-8}$ cm^3 s^{-1}. This effective value includes both radiative and nonradiative processes (upon weak pumping).

6. Conclusions

We have obtained the dependence of the mode gain on current from the experimental dependence of the threshold current on the cavity length in ultra-low-threshold laser diodes based on MBE-grown InAs/InGaAs QD structures. The minimum room-temperature lasing threshold is 16 A cm^{-2}. The gain in the ground-state band in the range from 1230 to 1250 nm asymptotically tends to its maximum value corresponding to the total population inversion of the working states. The average effective cross section related to the ground states of InAs QDs in the InGaAs quantum has been determined from the maximum gain to be of about 7×10^{-15} cm^2. We assume in this approximation that σ is the cross section for the interaction of emission with an atom-like QD and do not consider the QD volume. The quantum well is treated as an active medium containing QDs at a certain concentration.

Our theoretical model describes the gain as a function of current. It provides good agreement with experimental data

on the gain and allows us to find important parameters of the InAs QD such as the minimum inversion threshold (~ 13 A cm^{-2}) and the capture coefficient C for the carriers relaxing to the ground state ($\sim 2 \times 10^{-7}$ cm^3 s^{-1}). We believe that this model is adequate for the description of the low-pump level regime (below the total inverse population of the ground states).

Acknowledgements. The authors thank G A Smolyakov from Center for High Technology Materials, University of New Mexico for numerical calculations of the waveguide.

References

1. Arakawa Y, Sasaki H *Appl. Phys. Lett.* **40** 939 (1982)
2. Drakin A E, Eliseev P G *Sov. J. Quantum. Electron.* **14** 119 (1984)
3. Hirayama H, Matsunaga K, Asada K, Suematsu Y *Electron. Lett.* **30** 142 (1994)
4. Kirstaedter N, Ledentsov N N, Grundmann M, Bimberg D, Ustinov V M, Ruvimov S S, Maximov M V, Kop'ev P S, Alferov Zh I, Richter U, Werner P, Goesele U, Heydenreich J *Electron. Lett.* **30** 1416 (1994)
5. Liu G T, Stintz A, Li H, Malloy K J, Lester L F *Electron. Lett.* **35** 1163 (1999)
6. Lester L F, Stintz A, Li H, Newell T C, Pease E A, Fuchs B A, Malloy K *IEEE Photon. Technol. Lett.* **11** 931 (1999)
7. Asada M, Miyamoto Y, Suematsu Y *IEEE Quantum. Electron.* **22** 1915 (1986)
8. Mikai K, Ohtsuka N, Shoji H, Sugawara M *Appl. Phys. Lett.* **68** 3013 (1996)
9. Kirstaedter N, Schmidt O G, Ledentsov N N, Bimberg D, Ustinov V M, Egorov A Yu, Zhukov A E, Maximov M V, Kop'ev P S, Alferov Zh I *Appl. Phys. Lett.* **69** 1226 (1996)
10. Grundmann M, Bimberg D *Phys. Rev. B* **55** 9740 (1996)
11. Asryan V, Suris R A *Semicond. Sci. Technol.* **11** 554 (1996)
12. Zhukov A E, Kovsh A R, Ustinov V M, Egorov A Yu, Ledentsov N N, Tsatsul'nikov A F, Maximov M V., Shernyakov Yu M, Kopchatoiv V I, Lunev A V, Kop'ev P S, Bimberg D, Alferov Zh I *Semicond. Sci. Technol.* **14** 118 (1999)